

EMPLOYING A FAILURE CRITERION WITH INTERACTION TERMS TO SIMULATE THE PROGRESSIVE FAILURE OF CARBON-EPOXY LAMINATES

Jamaluddin Mahmud¹, A. Faris Ismail² and Tasneem Pervez³

¹Faculty of Mechanical Engineering, Universiti Teknologi MARA, 40450 UiTM, Shah Alam, Selangor, Malaysia

²Kulliyah of Engineering, International Islamic University Malaysia, Jalan Gombak, 53100 Kuala Lumpur, Malaysia

³College of Engineering, Sultan Qaboos University, P.O. Box 50, Muscat 123, Sultanate of Oman

ABSTRACT

A failure criterion with the existence of coupling terms is employed to investigate the progressive failure in anisotropic laminated carbon-epoxy plates. The criterion is employed because it is developed recently. Moreover, the criterion allows interaction between fiber and matrix properties. This paper is aimed to investigate the contribution of the coupling terms and thus, to simulate the progressive failure of the carbon-epoxy plates. A mathematical model and computational model are presented for the analysis. The deformation of the plates is predicted based on higher order shear deformation theory. Variation of material properties through thickness is used and accommodated by a discrete layer approach. A program based on finite element method is developed to determine the lamina stresses. Stresses calculated are used in the present failure model to determine the first ply failure and last ply failure, by progressively reducing the stiffness of the laminas. Finally, the first ply failure and last ply failure results are used to determine the lower and upper bounds within which the true load carrying capacity lies. The numerical results obtained show some improvement compared to other failure criteria.

Keywords : Failure Criteria, Composite Laminated Plate, FEA

1. INTRODUCTION

In conventional structures, it is sufficient to have the members that are made only of materials, which are usually considered as homogeneous and isotropic in design; however, modern structures such as in aircraft and aerospace industry would require more than that. Designing materials, which are strong and stiff yet light in weight, are desired. The search for a material, which is to be light and at the same time strong has resulted in the use of high strength, high modulus fibers reinforced in low strength, low modulus and low density matrix material, and thus leads to the development of composite materials. Such composites, idealised as orthotropic lamina, are bonded together to form a laminate and are used as structural components. Though the development of such fiber reinforced composite materials offers more variety in materials selection, it also increases the complexity in design and analysis, especially in ensuring the structure to perform without failure.

Unlike isotropic materials, composite materials demonstrate failure behaviour differently. In laminated composite materials, failure is distinguished by its mode of failure; which are the fiber failure in tension, matrix failure in tension, fiber failure in compression, matrix failure in compression and delamination. Failure in one direction of any single layer implies neither total failure of that layer, nor the whole structure. Load carrying capacity still exists not only in the structure, but also in the layer itself [1]. Therefore, the most common way to deal with failure of a composite laminate is by using two definitions of failure. First Ply Failure (FPF) occurs when initial failure of a single layer in a laminate fails in any

mode of failure. Last Ply Failure (LPF) occurs after the structure has degraded to the point where it is no longer capable of carrying additional load.

The present study is aimed to simulate and analyse the progressive failure of the plates from the initial failure, which is the First Ply Failure, up to the total failure, which is the Last Ply Failure. A failure criterion with the existence of coupling terms to determine the mode of failure for composite materials is employed. The uniqueness of this criterion compared to all other existing criteria which could determine mode of failure, is that it includes the coupling terms, which relate the interaction between the longitudinal and transverse stresses. As a consequence, it allows the interaction between the fiber properties and the matrix properties in terms of the strength of the material, which other failure criteria have neglected. The behaviour and the pattern of the progressive failure are studied. The results obtained with current failure criterion are then compared with the results obtained with existing failure criteria.

2. LITERATURE SURVEY

The most common and oldest method, in terms of finite element analysis for a laminated composite plate, is the standard laminate strength analysis [2]. However, the method neglects the local effects such as fiber misalignment, material discontinuities and free edge effects and assumes that the stiffness of the laminate receives no contribution from failed layers.

In 1982, Lee has performed the finite element based failure analysis by using his own direct mode determining failure

criterion [3]. The major drawback of a three-dimensional failure analysis is the tremendous amount of memory space and calculation time required. Later, improvement on the computational aspects of the three-dimensional formulation is done by other researchers [4,5]. However, the process is still found complicated to be implemented. This phenomenon leads to the search for more efficient finite element analysis of composite plates. Therefore, two-dimensional plate formulations for composite plates are then developed aggressively. Reddy and Pandey have developed a first ply failure analysis of composite laminates based on first order shear deformation plate theory [6]. The limiting factor of this analysis is the inadequacy of the first order shear deformation theory for thick composite plates. Engblom and Ochoa develop a two dimensional plate analysis to the above, but with increased interpolation in the through thickness direction [7,8]. Their analysis is carried out to the last ply failure. Tolson and Zabaraz have also developed two-dimensional progressive failure analysis of fiber reinforced laminated composite plates using higher order shear deformation theory [2]. Lee's [3] and Hashin's [9] failure criteria are used to determine the mode of failure, so that stiffness reduction could be done up to the last ply failure. However, both criteria neglect the interaction of the coupling effect between the longitudinal stress and the transverse stress. The coupling terms are completely absent in all the equations for both criteria. Therefore, the objective of this paper is to develop and simulate a two-dimensional finite element progressive failure analysis of carbon fiber reinforced laminated composite plates by employing a failure criterion with interaction terms and later, investigate the contribution of the coupling terms based on the failure curves.

3. HIGH ORDER SHEAR DEFORMATION

Higher order shear deformation theory is developed to improve both the classical lamination theory and the first order shear deformation theory by removing the assumption that a line which is originally straight and perpendicular to the middle surface remains straight when the laminate is extended or bent. A higher order term is included in the assumed displacements to describe the warping effect. According to the High-Order Shear Deformation Lamination Theory [10], the assumed displacements are as follows:

$$u(x, y, z) = u_0(x, y) - z\theta_x(x, y) + z^3\xi_x(x, y) \quad (1)$$

$$v(x, y, z) = v_0(x, y) - z\theta_y(x, y) + z^3\xi_y(x, y) \quad (2)$$

$$w(x, y, z) = w_0(x, y) \quad (3)$$

where, u , v and w , are the laminate displacements in the x -, y - and z -directions respectively. u_0 , v_0 and w_0 refers to the middle surface displacements. θ_x and θ_y refers to the bending slope in the x - and y - axes respectively, while ξ_x and ξ_y refers to the warping slopes. The strains are then written in vector form as in Equation (4).

$$\begin{Bmatrix} \varepsilon_x \\ \varepsilon_y \\ \gamma_{xy} \end{Bmatrix} = \begin{Bmatrix} \frac{\partial u_0}{\partial x} \\ \frac{\partial v_0}{\partial y} \\ \frac{\partial u_0}{\partial y} + \frac{\partial v_0}{\partial x} \end{Bmatrix} - z \begin{Bmatrix} \frac{\partial \theta_x}{\partial x} \\ \frac{\partial \theta_y}{\partial y} \\ \frac{\partial \theta_x}{\partial y} + \frac{\partial \theta_y}{\partial x} \end{Bmatrix} + z^3 \begin{Bmatrix} \frac{\partial \xi_x}{\partial x} \\ \frac{\partial \xi_y}{\partial y} \\ \frac{\partial \xi_x}{\partial y} + \frac{\partial \xi_y}{\partial x} \end{Bmatrix} \quad (4)$$

ε_x and ε_y are the normal strains in the x - and y - directions respectively. γ_{xy} is the shear strain in the xy -plane. The transverse shear strains could be written in vector form and shown in Equation (5).

$$\begin{Bmatrix} \gamma_{xz} \\ \gamma_{yz} \end{Bmatrix} = \begin{Bmatrix} \frac{\partial w_0}{\partial x} - \theta_x \\ \frac{\partial w_0}{\partial y} - \theta_y \end{Bmatrix} + 3z^2 \begin{Bmatrix} \xi_x \\ \xi_y \end{Bmatrix} \quad (5)$$

These strains, ε_x , ε_y , γ_{xy} , γ_{xz} and γ_{yz} , are then substituted into Equation (6) and Equation (7) to calculate the stresses.

$$\begin{Bmatrix} \sigma_x \\ \sigma_y \\ \tau_{xy} \end{Bmatrix}_k = \begin{bmatrix} \bar{Q} \\ \bar{Q} \\ \bar{Q} \end{bmatrix}_k \begin{Bmatrix} \varepsilon_x \\ \varepsilon_y \\ \gamma_{xy} \end{Bmatrix} \quad (6)$$

$$\begin{Bmatrix} \tau_{xz} \\ \tau_{yz} \end{Bmatrix}_k = \begin{bmatrix} \bar{Q} \\ \bar{Q} \end{bmatrix}_k \begin{Bmatrix} \gamma_{xz} \\ \gamma_{yz} \end{Bmatrix} \quad (7)$$

The symbols, σ_x and σ_y , are the normal stresses in the x - and y - axes respectively, while τ_{xy} is the shear stress in the xy -plane. τ_{xz} and τ_{yz} are the transverse shear stresses. k refers to the k th layer of the laminate. The $[\bar{Q}]$ is the transformed reduced matrix and its elements, \bar{Q}_{ij} , are given in terms of the reduced stiffnesses, Q_{ij} . The reduced stiffnesses, Q_{ij} are defined in terms of engineering constants [1]. These formulations are used in the finite-element program to determine the strains and stresses for the laminate analysis.

4. ALGORITHM

To determine the strength of a laminated plate, an incremental load analysis procedure is employed. For a given load, the stresses in each lamina can be calculated. Then the stresses in the material coordinates system are calculated. These stresses are then inserted into the failure criterion to determine if failure has occurred within a lamina of any element. If no failure occurs, the load would be increased to initiate the first failure. If failure occurs in the initial load, the analysis could be restarted at a lower initial load. When the first ply failure occurs, the stiffness is modified according to the mode of failure.

In the analysis done, the plate model is meshed into sixteen (4x4) uniform rectangular elements and each element has four Gauss points. The failure is checked for one by one layer of a Gauss point in an element. Therefore, altogether there are 256

points checked for matrix or fiber failure, where else, 192 points are checked for delamination. A fiber mode failure at a Gauss point of an element would reduce the stiffness matrix of the failed lamina within that element. Consequently, Q_{11} , Q_{12} , Q_{16} , Q_{55} (σ_L , σ_{LZ} , σ_{LT}) would be reduced to zero for the failed lamina. If failure were detected at less than four Gauss points, the appropriate stiffness components would be reduced to zero for that element. Since, the total element stiffness is calculated from the summation of the stiffness contributed of all the Gauss points in that element, the failure occurs in more than one Gauss point, will have a greater impact on the total stiffness of that particular element.

A matrix failure at a Gauss point of an element would reduce the stiffness for that element in a different manner. Q_{22} , Q_{12} , Q_{16} , Q_{44} (σ_T , σ_{TZ} , σ_{LT}) would be reduced to zero for this failed lamina. Again, if failure were to occur at 1, 2 or 3 Gauss points, the stiffness matrices would be reduced accordingly for that Gauss points and consequently, the stiffness of that element would reduce accordingly.

Delamination is the final mode of failure. It is characterised by the interlaminar stresses acting between adjacent layers. An interface of two adjacent layers is identified as delamination failure if either

$$\frac{\sigma_3}{Y} = 1 \quad \text{or} \quad \frac{(\sigma_5^2 + \sigma_4^2)^{1/2}}{S_z} = 1 \quad (8)$$

where S_z is the through-thickness shear strength [11]. A delamination failure at a Gauss point of an element would have yet another effect on the stiffness matrix. For both laminas adjacent to the delamination, Q_{33} , Q_{44} , Q_{55} (σ_z , σ_{TZ} , σ_{LZ}) are reduced to zero in both laminas adjacent to the failed interface. Obviously, when all the members of the element stiffness matrix have been reduced to zero the elements make no further contribution to the structure and is considered to have undergone total failure.

The composite analysis program is written to carry out the required calculations. It stores the lamina stiffness properties. For each element, an array is assigned to carry the information of the failure result for specific layer number and Gauss point location. Therefore, based on that information, stiffness properties can be reduced one at a time, appropriately as failure of the specific location is determined. The reduced material property matrices in global coordinates, Q_{ij} , must be recalculated every time new stresses are calculated to insure that the stresses take the failed lamina into effect. Once the new material stiffness matrices are calculated for each element, the elemental stiffness is then calculated for all the elements. The stresses are recalculated at this first ply failure (FPF) load using the newly calculated element stiffness matrices. These new sets of stresses are once again inserted into the failure criteria to check whether further failure will occur. If further failure happens, the stiffness is reduced appropriately and the stresses are recalculated once again at the FPF load. These 'equilibrium iterations' continue until no further failures occur at that particular FPF load.

If no further failure occurs, the load is incremented for the second time. Again, the stresses are calculated, and the laminate is checked for failure. Stiffness reduction and load increment continue until the stiffness matrix has been reduced to zero for all laminas at a single (x,y) location. This is considered to constitute last ply failure (LPF) or the ultimate strength. A flow chart of the algorithm described is given in Figure 1.

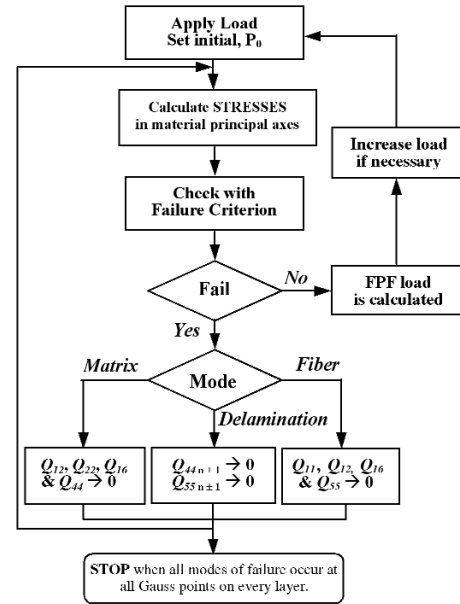


Figure 1: Flow chart diagram of the procedure for the progressive failure analysis

5. FAILURE MODEL

5.1 Fiber mode failure in tension

Considering transversely isotropic material [1], the equation used to determine the tensile failure in fiber mode is

$$\left(1 + A\right) \frac{\sigma_1}{X_T} - \frac{\sqrt{AB}}{X_T Y_T} (\sigma_1 \sigma_2 + \sigma_1 \sigma_3) - A \left(\frac{\sigma_1}{X_T}\right)^2 + \frac{1}{S^2} (\tau_5^2 + \tau_6^2) = 1 \quad (9)$$

$$\text{where } A = \frac{X_T}{X_C} \text{ and } B = \frac{Y_T}{Y_C}.$$

In equations (9) to (12), the meaning of the symbols is explained as below:

σ_1 , the longitudinal stress in 1-direction

σ_2 , the normal stress in 2-direction

σ_3 , the normal stress in 3-direction

τ_4 , the shear stress in 23-plane

τ_5 , the shear stress in 31-plane

τ_6 , the shear stress in 12-plane

1,2,3 refers to the axes in the principal material coordinates, where 1-direction is associated with the fiber direction.

X_T , axial or longitudinal strength in tension

X_C , axial or longitudinal strength in compression

Y_T , transverse strength in tension

Y_C , transverse strength in compression

S , shear strength

5.2 Matrix mode failure in tension

Considering transversely isotropic material [1], the equation used to determine the tensile failure in matrix mode is

$$(1+B)\frac{(\sigma_2+\sigma_3)}{Y_T} - \frac{\sqrt{AB}}{X_T Y_T}(\sigma_1\sigma_2 + \sigma_1\sigma_3) - \frac{B}{Y_T^2}(\sigma_2+\sigma_3)^2 + \frac{\tau_4^2}{R^2} + \frac{1}{S^2}(\tau_5^2 + \tau_6^2) = 1 \quad (10)$$

5.3 Fiber mode failure in compression

Considering transversely isotropic material [1], the equation used to determine the compressive failure in fiber mode is

$$\sigma_1 = X_c \quad (11)$$

5.4 Matrix mode failure in compression

Considering transversely isotropic material [1], the equation used to determine the compressive failure in matrix mode is

$$\left(\frac{1+B}{B}\right)\left(\frac{\sigma_2+\sigma_3}{Y_C}\right) - \frac{1}{\sqrt{AB}}\left(\frac{\sigma_1\sigma_2 + \sigma_1\sigma_3}{X_C Y_C}\right) - \frac{1}{B Y_C^2}(\sigma_2+\sigma_3)^2 + \frac{\tau_4^2}{R^2} + \frac{1}{S^2}(\tau_5^2 + \tau_6^2) = 1 \quad (12)$$

6. COMPARISON OF THE NUMERICAL SOLUTION TO EXACT SOLUTION

To validate the finite-element computer program developed, the current finite-element formulation is compared with classical plate theory, three dimensional elasticity formulation and other finite element formulations. The computer program is used to determine the stresses distribution of a 0/90/90/0 laminated composite plate subjected to a sinusoidally distributed transverse load as equation below;

$$P = P_0(\sin\pi x/a)(\sin\pi y/a) \quad (13)$$

The orthotropic material properties used for the comparison are those of a graphite/epoxy compound as below;

$$E_1 = 25 \times 10^6 \text{ psi}$$

$$E_2 = 1 \times 10^6 \text{ psi}$$

$$\nu_{12} = 0.25$$

$$\nu_{13} = 0.25$$

$$\nu_{23} = 0.25$$

$$G_{12} = 0.5 \times 10^6 \text{ psi}$$

$$G_{13} = 0.5 \times 10^6 \text{ psi}$$

$$G_{23} = 0.2 \times 10^6 \text{ psi}$$

Table 1. Normalised displacements for a 0/90/90/0 plate under sinusoidal transverse pressure

Span to thickness ratio, S	Source	Central deflection $w^*\left(\frac{a}{2}, \frac{a}{2}, 0\right)$
4	A – Present finite-element formulation	4.411
	B – Exact elasticity solution[12]	4.491
	C – FE formulation of Panda et al[4]	-
	D – FE formulation of Tolson et al[2]	4.393
10	A – Present finite-element formulation	1.671
	B – Exact elasticity solution[12]	1.709
	C – FE formulation of Panda et al[4]	1.448
	D – FE formulation of Tolson et al[2]	1.671
20	A – Present finite-element formulation	1.178
	B – Exact elasticity solution[12]	1.189
	C – FE formulation of Panda et al[4]	1.114
	D – FE formulation of Tolson et al[2]	1.177
50	A – Present finite-element formulation	1.029
	B – Exact elasticity solution[12]	1.031
	C – FE formulation of Panda et al[4]	1.016
	D – FE formulation of Tolson et al[2]	1.026
100	A – Present finite-element formulation	1.007
	B – Exact elasticity solution[12]	1.008
	C – FE formulation of Panda et al[4]	1.003
	D – FE formulation of Tolson et al[2]	1.006
	E – Classical Plate Theory[2]	1.000

All plates analysed are square with planar dimension $a \times a$, and total thickness, h . The plate is meshed into sixteen (4 x 4) uniform rectangular elements. Eight-noded element is used throughout the calculations. The origin of the plate is located at the lower left corner of the midplane.

The plate is simply supported and the boundary conditions used are as follows;

$$\begin{aligned} v(x, a/2) = \theta_y(x, a/2) = \xi_y(x, a/2) = 0 \\ u(a/2, y) = \theta_x(a/2, y) = \xi_x(a/2, y) = 0 \\ v(0, y) = w(0, y) = \theta_y(0, y) = \xi_y(0, y) = 0 \\ u(x, 0) = w(x, 0) = \theta_x(x, 0) = \xi_x(x, 0) = 0 \end{aligned}$$

Tabulated results for displacements are presented in Table 1, while results for stresses distributions are presented in Table 2.

The displacements and stresses reported are stated in their normalised form. This is done to remove the effects of varying loads and changing aspect ratios, $S = a/h$. The normalising equations used are as follows:

$$w^* = \frac{w\pi^4\alpha}{12q_0hS^4} \tag{14}$$

where

$$\alpha = \frac{4G_{12} + \{E_1 + E_2(1 + 2\nu_{12})\}}{(1 - \nu_{12}\nu_{21})} \tag{15}$$

$$\sigma_x^* = \frac{\sigma_x}{P_0S^2} \tag{16}$$

$$\sigma_y^* = \frac{\sigma_y}{P_0S^2} \tag{17}$$

$$\sigma_{xy}^* = \frac{\sigma_{xy}}{P_0S^2} \tag{18}$$

$$\sigma_{xz}^* = \frac{\sigma_{xz}}{P_0S} \tag{19}$$

$$\sigma_{yz}^* = \frac{\sigma_{yz}}{P_0S} \tag{20}$$

P_0 is the maximum value pressure load applied on top of the surface.

A detail analysis is done for the case where the aspect ratio of the plate, $S = 10$. Tabulated results for the stresses distributions are presented in Table 2. Stresses reported are stated in their normalised form. This is done to compare with other results obtained by other researchers.

The column with the title ‘Source’ indicates the source of the results displayed in Table 2. The letter B, C and D used are the same source as used in Table 1. The letter B is representing the exact elasticity solution as given by Pagano and Hatfield [12]. Letter C represents the results obtained by Panda and Natarajan [4]. Letter D represents the results obtained by Tolson and Zabaraz [2] for four by four (4x4) elements. Letter E refers to the solutions obtained using Classical Lamination Theory [2]. Table 2 obviously proves that the stresses obtained using the finite-element program developed are close to the exact solution.

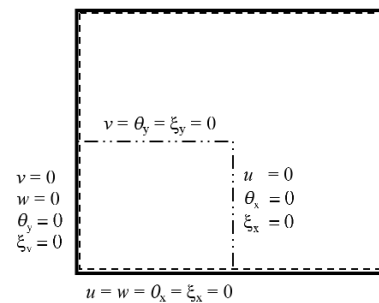


Figure 2: The boundary condition for quarter of a square plate

7. PROGRESSIVE FAILURE OF A PLATE UNDER TRANSVERSE LOADING

The computer program is used to investigate the first ply and last ply failure loads of a 0/90/90/0 laminated composite plate [1]. The plate is subjected to a sinusoidally distributed transverse load where $P = P_0(\sin\pi x/a)(\sin\pi y/a)$. The plate is square with the dimensions of $a \times a$. The thickness of the plate is h , with the aspect ratio, $S = a/h$. The analysis is performed on different aspect ratios. The aspect ratio is varied from 5 to 100. Two sets of dimensions is used to increase the analysis reliability. The first dimensioning of the analysis is carried out in metric system. The length of the plate is 40 mm. The second set of analysis is carried out with the length of the plate is 2 inches. Only a quarter of the plate needs to be modelled due to the geometric symmetry of the problem [6]. The plate is simply supported and the boundary conditions used are as in Figure 2.

Table 2. Normalised stresses for a simply supported 0/90/90/0 square plate

S	Source	$\sigma_x^*\left(\frac{a}{2}, \frac{a}{2}, \frac{h}{2}\right)$	$\sigma_y^*\left(\frac{a}{2}, \frac{a}{2}, \frac{h}{4}\right)$	$\sigma_{xy}^*\left(0, 0, \frac{h}{2}\right)$	$\sigma_{xz}^*\left(0, \frac{a}{2}, 0\right)$	$\sigma_{yz}^*\left(\frac{a}{2}, 0, 0\right)$
10	A	0.600	0.390	0.0276	0.284	0.174
	B	0.559	0.403	0.0276	0.301	0.196
	C	0.532	0.307	0.0250	-	-
	D	0.575	0.401	0.0280	0.299	0.191

The material and strength properties for the carbon-epoxy composite used [1,2] are shown below. Sixteen eight-noded elements are used to insure reasonable accuracy in stress calculations. The progressive failure analysis is performed using the present failure criterion. Lee failure criterion is used as a comparison.

E_1	=	180 GPa
E_2	=	10.6 GPa
E_3	=	10.6 GPa
$\nu_{12}=\nu_{13}$	=	0.28
ν_{23}	=	0.28
$G_{12} = G_{13}$	=	7.56 GPa
G_{23}	=	7.56 GPa
X_T	=	1500 MPa
X_C	=	1500 MPa
Y_T	=	40 MPa
Y_C	=	250 MPa
S_A	=	68 MPa
S_T	=	68 MPa
S_Z	=	68 MPa

To ensure the results are converging and accurate, two sets of simulation are done [1]. The first analysis is performed with the dimensions of the plate length, $a = 2$ inches and the material properties used are in pound per square inch, psi. Second analysis is carried out in the metric dimensioning system. This is done to see the reliability of the normalised equation in calculating the normalised First Ply Failure Load, FPF* and the normalised Last Ply failure load, LPF*, with respect to the aspect ratio, S . Therefore, the material properties used are in N/m^2 (Pa). The length and width of the plate, a , under consideration is 40 mm (0.04 m).

8. RESULTS AND DISCUSSION

The results of the analysis are tabulated in Table 1 and Table 2. Figure 3 shows the first ply and last ply failure curves for the 0/90/90/0 laminated as a function of aspect ratio. The failure loads in the graph have been normalised as

$$FPF^* = (FPF)S^2/10^6 \quad (21)$$

$$\text{and } LPF^* = (LPF)S^2/10^6 \quad (22)$$

Table 3a. FPF loads using present failure criterion

Aspect Ratio, S	5	10	20	50	100
Ply thickness, t_i (mm)	2	1	0.5	0.2	0.1
Unnormalised FPF Load (MPa)	41.7	16.0	4.3	0.7	0.18
Normalised Load, FPF* (MPa)	1044	1603	1732	1758	1764

Table 3b. LPF loads using present failure criterion

Aspect Ratio, S	5	10	20	50	100
Ply thickness, t_i (mm)	2	1	0.5	0.2	0.1
Unnormalised LPF Load (MPa)	41.7	19.5	6.0	1.0	0.26
Normalised Load, LPF* (MPa)	1048	1956	2415	2600	2640

Table 3a and 3b display the exact values of the FPF load and LPF load as well as the normalised loads. The title 'Present Failure Criterion' indicates that the data in the table are determined using the present failure criterion. The title 'Aspect Ratio, S ' refers to the aspect ratio of the plate analysed. 'Ply thickness, t_i ' indicates the thickness of each ply in the laminate. For the analysis performed in the S.I. unit, the thickness of each ply is given in millimetre while for the analysis performed in the U.S. customary unit, the thickness is given in inches. 'Unnormalised Load' refers to the actual FPF or LPF load, P_o , applied in the analysis. The load could be applied in Pascal or psi depending on the analysis. The 'normalised load' is the load calculated using the normalising equations as in Equations (21) and (22).

The normalised FPF loads, FPF* and LPF loads, LPF*, in Table 3 are plotted against the aspect ratio and the graphs are shown in Figure 3. The graphs are plotted in such a way to compare with the existing results [2]. In general, the graphs reveal the same behaviour of the progressive failure. The results shown in Figure 3 converge for the LPF curve but the FPF curve maintains an equal percent difference throughout. It is interesting to observe that for the aspect ratio less than 12, the last ply failure loads using the Lee criterion are lower than the last ply failure loads using the present criterion. Overall results show that the FPF and LPF boundary using the present criterion are inbound when compared to the FPF and LPF boundary using the Lee criterion. This is due to the coupling terms in the present criterion, where the interaction of the stresses in the longitudinal and transverse direction has improved the boundary of the FPF and LPF of the laminate. The interaction of the stresses has enabled the stresses in the transverse direction to produce an effect to the stresses in the longitudinal direction. A phenomenon of compensating each other has taken place, which balanced the difference in longitudinal and transverse stresses, as well as the strength in both directions. The interaction terms have allowed interaction of the fiber and matrix strength, as well as the tensile and compressive strength. Therefore, unlike other failure criteria, the present criterion does not allow independent failure mode based on only one direction. It has created a dependency and effect of the longitudinal stresses on the transverse stresses, and vice versa. The interaction has improved the failure boundary by upgrading the FPF limit. However, as a consequence, the interaction has also decreased the LPF limit.

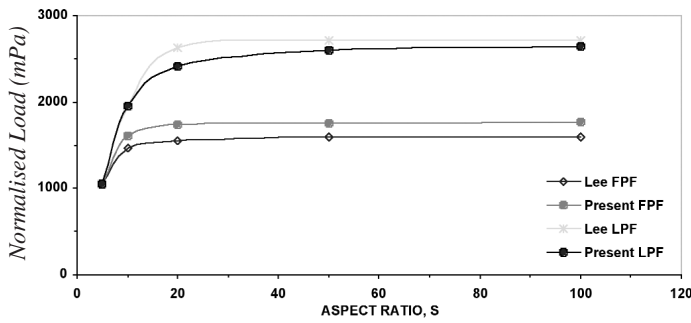


Figure 3: Normalised first ply failure and last ply failure load

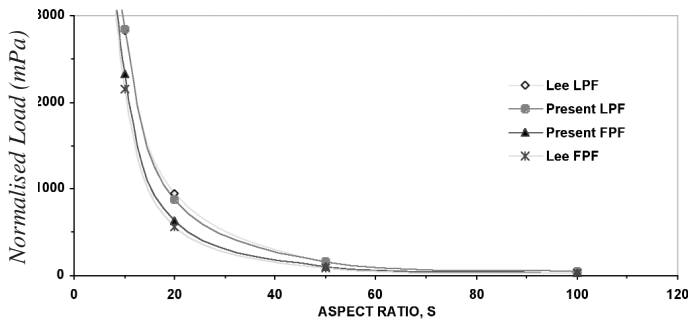


Figure 4: First ply failure and last ply failure load

As a whole, it has made the limit of FPF and LPF a smaller region and which is more realistic and reliable in term of the laminate strength.

Figure 4 shows the graphs for the non-normalised load with respect to the aspect ratio, S . The distributed load is in psi and applied to a plate with the width, $a = 2$ inches. In order to enlarge the graphs for better observation, the figure is focused on the aspect ratio larger than 10. The actual load applied for $S = 5$ is not shown in the diagram. From the graphs, it is clear that as the aspect ratio increase, the boundary region of the FPF and LPF gets smaller, except at $S = 10$, where the FPF and LPF limit falls on the same point. The reason for this to happen is because the first mode of failure that occur for a plate with the aspect ratio, $S = 10$ is delamination. This is true because a laminate, which is constructed from thick laminas, will tend to delaminate as compared to a laminate, which is constructed from thin laminas. From the analysis done, for a plate with aspect ratio equal and greater than 10, the first mode of failure that occur is the tensile matrix failure. Figure 4 also shows that for a plate with aspect ratio, S , beyond 100, the FPF and LPF load will converge to a point. The maximum boundary region of the lower limit, FPF and upper limit, LPF happens when $S = 10$ to 20. Therefore, for a plate with aspect ratio 10 to 20, an average of another 30 percent load could be applied after the first failure occurs. Another thing that could be observed from the graphs is that the distributed load, P_0 , decreases exponentially as the aspect ratio, S , increases.

Figures 5a through 6d show the progression of failure within the 0/90/90/0 laminated plate with $S = 50$ using the present failure criterion. No such detail progressive failure has been presented for a plate with an aspect ratio of 50. Moreover, these results are determined using the present failure criterion, which means that the present failure criteria are used to simulate the progressive failure of the plate. As shown in

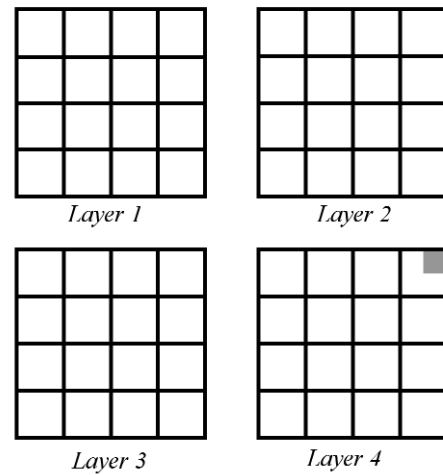


Figure 5a: Failure progression of a 0/90/90/0 plate under transverse sinusoidal load (FPF – normalised load 1772 MPa)

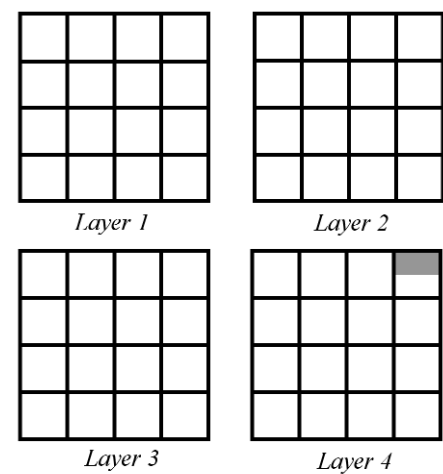


Figure 5b: Failure progression of a 0/90/90/0 plate under transverse sinusoidal load (after equilibrium iteration – normalised load 1772 MPa)

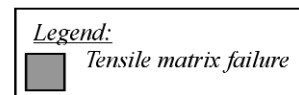


Figure 5a, the failure occurs in the area closest to the centre of the plate at the bottom 0° lamina. The initial failure is matrix mode caused by tensile stresses. To be exact, the initial failure that occurs is a tensile matrix failure and the location is on the layer number 4 of the sixteenth element at the fourth Gauss point of the plate.

When the normalised load applied is increased to 1772 MPa, the matrix failure progressed to the next Gauss Point of element 16 at the bottom of the 0° lamina. At this FPF* value, after the first ‘equilibrium iteration’ is done, the initial matrix failure has progressed to its neighbour that is the Gauss point number 2, as shown in Figure 5b. This is a typical example of a progressive failure that occurs in a composite laminate. We could observe in Figure 5b that the pattern of the failure is not symmetry. In the sixteenth element on layer number 4, Gauss point number 2 and Gauss point number 4 have undergone tensile matrix failure but Gauss point number 3 has not been affected.

EMPLOYING A FAILURE CRITERION WITH INTERACTION TERMS TO SIMULATE THE PROGRESSIVE FAILURE OF CARBON-EPOXY LAMINATES

Figures 6a to 6d show a more aggressive example of the progressive failure, which leads to total failure of the same carbon-epoxy composite plate. The step-by-step presentation of the progressive failure that occurs, when the plate is subjected to a normalised load of 2600 MPa, is displayed in detail. As we could observe in Figure 6a, when the applied load is increased to 2600 MPa (normalised unit), additional failure occurs on the plate as compared to Figure 5. At this normalised FPF load, layer 4 has undergone severe matrix mode failure caused by tensile stresses. At the same time, fiber mode failure caused by tensile stresses has occurred in the first element of layer 1 and layer 4. Figure 6a also shows clearly that layer 2 and layer 3, which is the inner layer of the plate and bounded by layer 1 and layer 4, have not been affected at all.

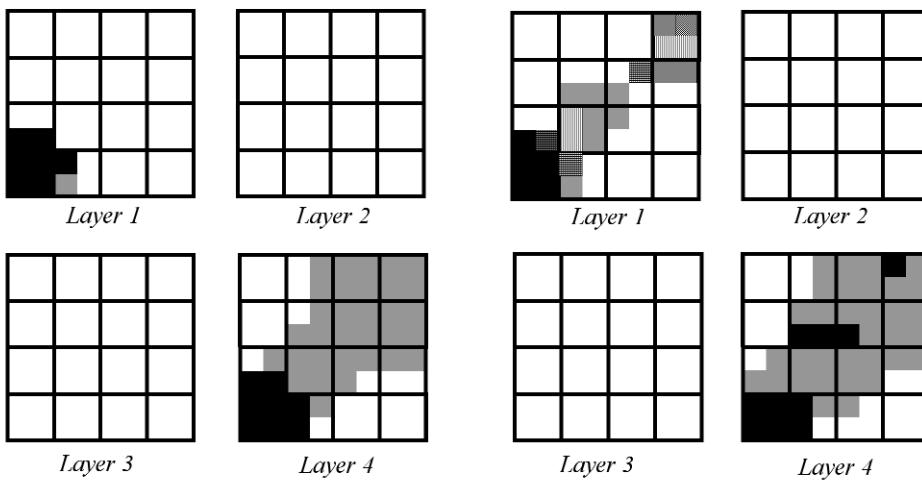


Figure 6a: Failure progression of a 0/90/90/0 plate under transverse sinusoidal load (FPF – normalised load 2600MPa)

However, after the first equilibrium iteration, as shown in Figure 6b, element 1 in layer 1 undergone failure in matrix mode and fiber mode caused by tensile stresses, as well as fiber mode failure caused by compressive stresses. At this instant, a fiber mode failure caused by compressive stresses has initiated at the area closest to the centre of the plate in layer 1.

After the second equilibrium iteration, as shown in Figure 6c, failure has progressed significantly in layer 1. Various mode of failure has occurred in layer 1. In layer 4, matrix mode and fiber mode failure caused by tensile stresses widespread to three-quarter of the layer. However, at this instant, layer 2 and layer 3 have still not been affected.

Figure 6d shows the failure region after the third equilibrium iteration for the normalised FPF load at 2600 MPa.

It is obvious that layer 1 has undergone severe failure. The diagonal elements of layer 1 have undergone total failure. Various mode of failure has widespread to three-quarter of the layer. Layer 4 has also undergone severe matrix and fiber mode failure caused by tensile stresses. It is interesting to note that after the third equilibrium iteration, failure progresses to layer 2 and layer 3. Layer 2 experiences severe failure, whereby the diagonal region fails totally, while failure in matrix mode caused by the tensile stresses progresses rapidly.

Figure 6d also shows that failure in matrix and fiber mode caused by tensile stresses has initiated and widespread rapidly in layer 3. It is interesting to observe that layer 3 and layer 4, which is the two layers at the bottom of the laminate, at this moment, have only experienced matrix and fiber mode failure caused by the tensile stresses. The top two layers, which are layer 1 and layer 2, experience various mode of failure that causes the diagonal region to fail totally. This shows that the two layers below the mid-plane of the plate, is dominantly under the tensile state of stress and this is causing the severe tensile failure.

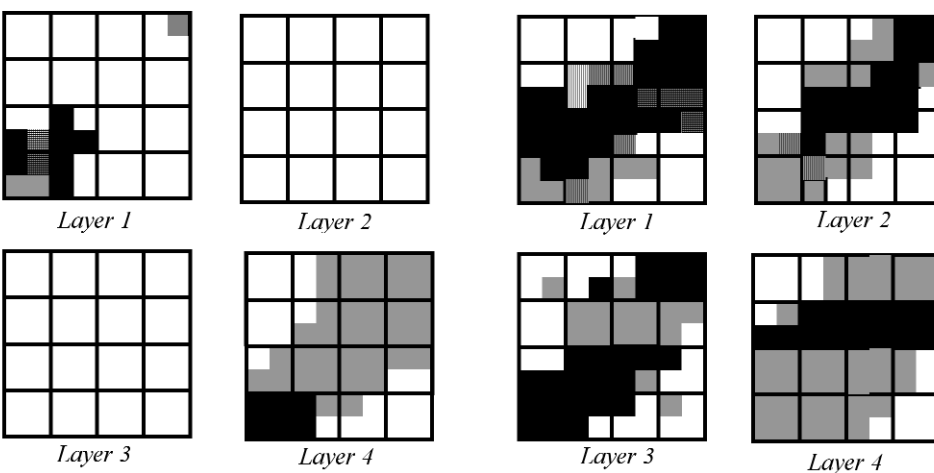
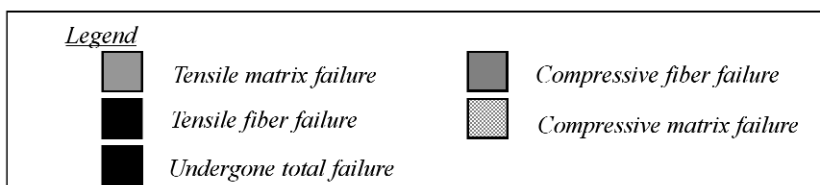


Figure 6b: Failure progression of a 0/90/90/0 plate under transverse sinusoidal load (After first equilibrium iteration – normalised load 2600MPa)

Figure 6c: Failure progression of a 0/90/90/0 plate under transverse sinusoidal load (After second equilibrium iteration – normalised load 2600MPa)

Figure 6d: Failure progression of a 0/90/90/0 plate under transverse sinusoidal load (After third equilibrium iteration – normalised load 2600MPa)



8. CONCLUSION

The main objective to simulate the progressive failure of fiber reinforced carbon-epoxy plates has been achieved successfully. As forecasted, the results obtained show that the present failure criterion with the existence of coupling terms, improve the prediction of the progressive failure. The results are

more realistic and reliable. Furthermore, the validation of the results compared to analytical result, experiment and other computational results ensures its accuracy.

The discussion on the results of this analysis, supported by figures and the explanation of each figure in this section, is hoped to give a better understanding on the progressive failure of the 0/90/90/0 carbon-epoxy composite laminate. The tabulated results as well as the graphs are presented in such that they could be used as future references.

The work done is hoped to give a better understanding on how a fiber reinforced composite laminate fails, and more importantly the behaviour of the progressive failure. The study will help engineers to design an optimum fiber reinforced composite laminate that could withstand desired service and load condition. The beauty of the progressive failure of a composite laminate is that it allows the laminate to withstand the load even after FPF as long as the load applied does not exceed the ultimate LFP load. Moreover, it also allows us to predict when the laminate will fail totally. A comprehensive understanding of the progressive failure behaviour of the laminates will make us appreciate the service that fiber reinforced composite laminates could offer in our structural design and applications. ■

REFERENCES

- [1] J. Mahmud, *Failure Analysis of Composite Materials*, Master's Thesis, International Islamic University, Malaysia, 2002.
- [2] S. Tolson and N. Zabaraz, "Finite Element Analysis of Progressive Failure in Laminated Composite Plate", *Computers and Structures*, Vol. 38, pp. 361-372, 1991.
- [3] J.D. Lee, "Three Dimensional Finite Element Analysis of Damage Accumulation in Composite Laminate", *Computers and Structures*, Vol. 15, No. 3, pp. 335-350, 1982.
- [4] S.C. Panda and R. Natarajan, "Finite Element Analysis of Laminated Composite Plates", *International Journal for Numerical Methods in Engineering*, Vol. 14: pp. 69-79, 1979.
- [5] W.C. Hwang and C.T. Sun, "Failure Analysis of Laminated Composites by Using Iterative Three-Dimensional Finite Element Method", *Computers and Structures*, Vol. 33, pp. 41-47, 1989.
- [6] J.N. Reddy and A.K. Pandey, "A First-Ply Failure Analysis of Composite Laminates", *Computers and Structures*, Vol. 25, pp. 371-393, 1987.
- [7] J.J. Engblom and O.O. Ochoa, "Finite Element Formulation Including Interlaminar Stress Calculation", *Computers and Structures*, Vol. 23, pp. 241-249, 1986.
- [8] J.J. Engblom and O.O. Ochoa, "Analysis of Progressive Failure in Composites", *Composite Science and Technology*, Vol. 28, pp. 87-102, 1987.
- [9] Z. Hashin, "Failure Criteria for Unidirectional Fiber Composites", *Journal of Applied Mechanics*, Vol. 47, pp. 329-334, 1980.
- [10] T. Pervez, *Transient Dynamic, Damping and Elasto-plastic Analysis of Higher Order Laminated Anisotropic Composite Plates Using Finite Element Method*, Ph. D. Thesis, University of Minnesota, USA, 1991.
- [11] T. Pervez and M.A. Abul Fazal, "Progressive Failure Analysis of Laminated Composite Plates Based on Higher Order Shear Deformation Theory. Advances in Materials and Processing Technologies", *Proceeding of the Fourth International Conference (AMPT 1998)*, pp. 598-611, 1998.
- [12] N.J. Pagano and S.J. Hatfield, "Elastic behaviour of of multilayered bi-directional composites", *AIAA Journal*, No. 10, pp. 931-933, 1972.

BIOGRAPHY



JAMALUDDIN MAHMUD

Jamaluddin Mahmud has a B.Eng. (Hons.) Mechanical Engineering degree from Universiti Teknologi MARA (UiTM) and a MSc Manufacturing Engineering degree from

International Islamic University, Malaysia (IIUM). He joined the Faculty of Mechanical Engineering UiTM as a lecturer in 2001 and currently he is the Head for the Diploma in Mechanical Engineering program. He has three years of industrial experience, working as a service engineer in UMW Equipment Sdn. Bhd. Mr. Jamaluddin has been lecturing on Composite Materials, Finite Element Method, Manufacturing Processes and Product Design, which happens to be his areas of research interest and has published more than 20 technical papers in these areas in journals and conference proceedings. In the year 2004, one of his research project with Dr Wahyu Kuntjoro, has won the Best Fundamental Research Award in UiTM.



PROF. DR AHMAD FARIS ISMAIL

Prof. Dr. Ahmad Faris Ismail currently is a professor and the dean of faculty of engineering at International Islamic University Malaysia (IIUM). He obtained his Bachelor of Science in Chemical Engineering from University of Houston in 1988 before completing his Ph.D. from Rice University, U.S.A. in 1993. His research areas include simulation and modeling, energy systems, combustion, computational fluid dynamics, engineering mechanics, computer vision, and image processing. He has published more than 70 technical papers in these areas in international journals and conference proceedings.



ASSOC. PROF. DR TASNEEM PERVEZ

Tasneem Pervez has earned his Bachelor's degree in Mechanical Engineering from NED University of Engineering & Technology, and his MS and Ph.D. degrees from University of Minnesota, Minneapolis, USA in 1991. Currently he is working as an Associate Professor at Sultan Qaboos University, Oman. His current research interests are; Mechanics of laminated composite plates, Engineering Design and Analysis, FEM and Solid Expandable Tubular Technology.